MORSE: MESOSCALE OCEAN RADAR SIGNATURE EXPERIMENTS

G Connan[1], P Brennan[1], H D Griffiths[1], K Woodbridge[1]; L Leviandier[2]; W Alpers[3]; R Garello[4]; E Barthelemy[5], D Renouard[5]; J 0 Thomas[6], A C Edwards[6]

[1] University College London, United Kingdom; [2] Thomson-Marconi Sonar, France; [3] Universität Hamburg Institut für Meereskunde, Germany; [4] ENSTBr, France; [5] Université Joseph Fourier-Grenoble (LEGI), France; [6] Oxford Computer Services Ltd, United Kingdom

ABSTRACT

This paper describes work performed within the MORSE project as part of the EC MAST-III programme. Oceanic internal wave mechanism and effects are being studied by IfM and will be the basis for analysis of SAR images at ENSTB. The understanding of radar signatures requires the development by UCL of a laboratory W-band SAR using the FMCW technique. OCS will develop three software packages involving ocean parameter extraction, ocean surface modelling and the radar signature "inversion" problem. These packages are aimed at providing tools for those in the marine education, coastal engineering, marine technical services and oceanographic sciences The ultra high resolution radar is to be used in a set of experiments in LEGI, in Grenoble, France, first in a flume, and then in a wave tank in which scaled versions of particular internal wave phenomena can be set-up under laboratory conditions. This paper will particularly focus on the development of this radar.

1. INTRODUCTION

The MORSE project, which began in February 1996, endeavours to develop numerical models which are capable of predicting radar backscattering over all radar bands, of extracting ocean surface characteristics at high spatial resolution, of predicting internal wave fields in both time and space and of inverting radar signatures into geophysical parameters. Presently used models are not entirely reliable in producing *quantitative* results in terms of the 3-D hydrodynamic structure of the ocean. The aim of this work is to achieve progress in the understanding and mathematical description of the various processes involved in ocean imaging which, along with the increased processing power of modern computers, provides the opportunity for much more detailed and comprehensive models.

2. AIMS OF THE PROJECT

Since the US SEASAT mission, much understanding has been gained on the potential of SAR technology in oceanography. Ocean surface phenomena such as swells, surface slicks and island wind shadowing are readily visible on radar images. However, subsurface hydrodynamic phenomena (such as internal waves, internal tides, tidal currents and eddies) interact through complex processes with the surface wave field. Radar surface signatures will reflect these oceanic phenomena allowing the possibility of inferring such phenomena through very careful interpretation of the radar signature.

There are many diverse areas where information on subsurface hydrodynamic phenomena would be of great benefit, including off-shore drilling and mining, ship routing, fisheries and aqua culture, environmental monitoring, acoustic communication and detection and coastal engineering. Knowledge of wave conditions, on either an historical or real-time basis, will assist such fields by increasing the information relevant to the particular area of interest and also by reducing the costs and improving the safety of many operations.

Of course, to serve all these needs, appropriate software to extract information from radar images is required and to provide a real management tool, human intervention in the use of this software needs to be kept to a minimum. The purpose of this work is to contribute to the development of such precompetitive global tools. Although the ultimate goal is an integrated global management tool for ocean surveying, it is realised that this very ambitious objective will probably not be achieved within the three year timespan of this project. However, it is likely that an important step forward can be made and a breakthrough realised in the understanding and mathematical description of a number of basic hydrodynamic processes and radar imagery mechanisms along with their interactions. OCS will be focusing on modelling the strong perturbation of the ocean surface wave spectrum in the presence of 1-D steady straining currents - including those induced by non-linear internal waves. Three complex software packages will be stage-built; one (WASP) employing ENSTBr algorithms for extracting parameters from ocean imagery; a second (SWARM) based on OCSHIM (Oxford Computing Services Hydrodynamic Interaction Model) and IfM algorithms for generating wave spectra and modelling radar signatures; and a third (RADSIG) for matching modelled radar signatures to observed signatures, with the intent of establishing a route for using surface imagery to obtain information at depth.

Some of the new areas which are being studied in this work include:

1. Non-linear hydrodynamic interactions between internal waves and surface gravity waves/capillary waves, which are currently only partly known especially on experimental grounds;
2. A number of basic radar backscattering processes, especially for C-band (ERS-1) which are not completely taken into account in existing models;
3. Understanding of the main mechanisms involved in radar imaging by means of laboratory experiments involving the imaging of internal waves using a high resolution radar.

7th International Conference on Electronic Engineering in Oceanography, 23-25 June 1997, Conference Publication No 439 © IEE 1997

The effort involved in this work includes the development of a 94 GHz high resolution radar which will be used for a pilot study in the Coriolis turntable in Grenoble, expertise in image processing, physical oceanography and numerical simulation. The ultimate aim is to make possible the exciting and challenging task of processing radar images of ocean surfaces, in order to obtain accurate information on subsurface hydrodynamic phenomena.

3. OCEANIC INTERNAL WAVES

From a physical point of view, one of the striking characteristic properties of ocean radar images is the wide range of surface phenomena visible, which includes modulation of the sea surface roughness by internal waves. Image signatures assigned to long internal waves of large amplitudes have extensively been observed. Ocean internal waves are present on all levels of the water column in deep oceans as well as in marginal coastal seas. They range in wavelength from 10 centimetres to several kilometres. The processes of generation and dissipation have received considerable attention in the last 20 years. Amongst the variety of internal waves, very energetic waves are created by the tide interacting with the bottom bathymetry. These waves exhibit large length scales and are generally called long non-linear dispersive internal waves. They are generated at each tidal cycle and propagate towards the shore or also towards the open ocean ultimately breaking creating considerable mixing of the water column. These long internal waves are the ones clearly observable by remote sensing in coastal seas all over the world. They are also present in Europe, especially in the Mediterranean and in the Bay of Biscay.

It is worth noting that surface manifestations of internal waves are found in SAR images for moderate wind speeds and for any depth of water. It is well known since Alpers & Salusti (1) and Rufenach & Smith (2), that radar interaction seems a better way to detect and reveal internal waves than passive optical sensors such as LANDSAT.

3.1. Radar signatures of internal waves

As stated before, for other geographical phenomena imaged by SAR, the ability to show patterns related to internal waves over large portions of the ocean is fundamental. This advantage is paramount especially to those researchers who know and have experienced the difficulties of obtaining more than a few points of measurement with conventional techniques. One of the first examples of signatures of internal waves on SAR images was shown by Alpers and Salusti (1). The prominent features of ocean internal waves found on SAR images are as follows:

1. The waves are found in packets with sometimes more than 10 crests per group.
2. The crests/troughs are often linked to the bottom topography.
3. The waves appear either as dark against a light background (rough sea conditions) or light against a dark background (calm sea), and generally as dark and light bands showing that they can be imaged in a broad range of wind conditions.
4. The wavelength between individual light and dark bands is typically between several hundred metres and several kilometres, decreasing from the leading edge to the trailing edge.

It is now known that some of the radar signatures are associated with internal waves because these large waves produce significant modulations of the surface of the ocean. The real work of image understanding consists of extracting hard information, i.e. numbers of physical meaning, from the images. This 'hard' information consists of either parameters such as swell wavelengths or else as grey level distributions along transsects across image signatures (such as a train of internal waves). The spatial variation, if any, of measured swell wavelength can be interpreted as refraction caused by a change in bathymetry, variable surface current etc. A variation in a grey level distribution across an image signature is much more difficult to interpret and requires deep understanding of the physics of the ocean surface and its perturbation by unseen factors, e.g. bathymetry, internal waves. Figure 1 illustrates various hydrodynamic mechanisms linked with internal wave radar sensing.

The radar backscatter is influenced by velocity bunching, tilting and propagation direction. The modulations on the water surface arise from straining, shearing, refraction and resonant interaction of swells, wind waves, capillary waves and oil and natural slicks.

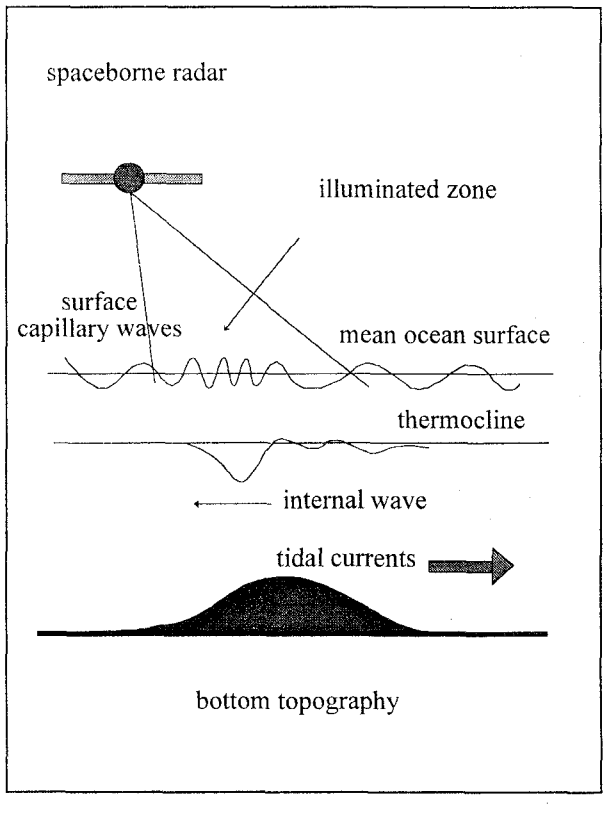

Figure 1: Radar internal wave imaging

3.2. Analysis of sea-surface SAR images

One of the aims of the project is to develop image processing methods able to provide a good characterisation of the ocean surface radar signatures of wave patterns. Concerning internal waves, one might notice that they are a non-stationary process localised in space. First, spectral analysis calculated on

short spans of data (small windows) can be performed using methods dedicated to that purpose, auto-regressive analysis, for instance (3). The technique is quite efficient but can be improved to take into account the variations in both space and frequency domains. The so-called Time-Frequency Decompositions (TFD) were the next method to be developed, and provide a better description of the wave packet wavelength with a good approximation of the wave energy (4). The TFD applied to wave fields, such as swell propagating near and towards the coast, yield a very fine determination of the wavelength and wave direction changes. Finally, due to their finite location in the image and their extent in the spatial frequency domain, internal waves are a well-suited phenomenon to be analysed by the Wavelet Transform. Quite good results can be achieved (5) for, first internal waves localisation (in space domain) and then the internal wave wavelength estimation (see paper by Rodenas and Garello in these proceedings).

4. RADAR DEVELOPMENT

The purpose of the laboratory W-band radar is to obtain radar imagery of water surface wave modulations in a wave flume or in a tank on the Coriolis turntable, LEGI, Grenoble, under particular wave conditions. It is thought that parasitic capillary waves which are generated by steep gravity waves will contribute to the modulation of the Bragg backscattering. In the tank or the flume, all wavelengths will be modulated by the internal wave current field. Therefore these short range experiments are also of some relevance for X-band and C-band radar and it will be interesting to test to what extent W-band works like X-band or C-band.

The required image size is taken to be 5 m x 5 m with a slant range resolution of 5 cm. The required radar bandwidth is related to the ground range resolution and the angle of incidence (or elevation angle) which is similar to that of a spaceborne SAR and is taken as 60°. This implies a radar bandwidth of some 3 GHz. In order to accommodate such bandwidth, a very high carrier frequency is necessary. Much radar hardware and technology exists at 94 GHz, both for radar seekers and for automotive radars. Such hardware is easily able to accommodate a bandwidth of 3 GHz, so the use of 94 GHz is a natural choice.

The FMCW technique is preferred to a pulsed radar since it permits high range resolution and high processing gain. At short range, this means that only a very low transmit power, and antenna gain, is necessary. To obtain equivalent azimuthal resolution implies the use of aperture synthesis techniques, with the radar moving along a circular arc in the case of the tank. Aperture synthesis has been shown to be compatible with the FMCW technique (6), and a practical radar of this kind has been built and demonstrated at University College London (7) (8).

4.1. Hardware design

The radar design is influenced by a number of factors, some of which are conflicting. This section outlines the major considerations involved in the design in a fairly logical order.

The position of the radar is constrained by the available space around the tank. We have found that the maximum radar height above the water surface is 2.5 m. Assuming it is mounted at a height of 2 m above the water surface, the geometry is as shown in Figure 2.

The required antenna beamwidth to provide full coverage of the swath is 43.3° (say 45°) and the range varies from 2.2 m to 6.3 m. The corresponding footprint is shown in Figure 3. The antenna gain associated with this beamwidth is of the order of 15 dBi, which requires an aperture of dimensions 7 mm x 5 mm at 94 GHz.

The range resolution is given by:

$$\Delta R = \frac{c}{2B\sin\theta}$$

where θ is the elevation angle of the radar, from which a sweep bandwidth, B, of 3 GHz gives roughly the range resolution required:

at inner edge of imaged area $\Delta R = 5.3$ cm;
at outer edge of imaged area $\Delta R = 11.2$ cm.

The SAR azimuth resolution is given by:

$$\Delta x = \frac{\lambda}{4\sin(\Delta\beta/2)}$$

where $\Delta\beta$ is the angular difference between a given point in the imaged area from one end of the synthetic aperture to the other. A SAR length of 1 m gives roughly the azimuth resolution required:

at inner edge: $\Delta\beta = 0.158$ rad and $\Delta x = 10$ mm;
at outer edge: $\Delta\beta = 0.447$ rad and $\Delta x = 3.6$ mm.

There is clearly a considerable variation in both azimuth and range resolutions across the imaged area, which is inevitable in view of the geometry of the arrangement.

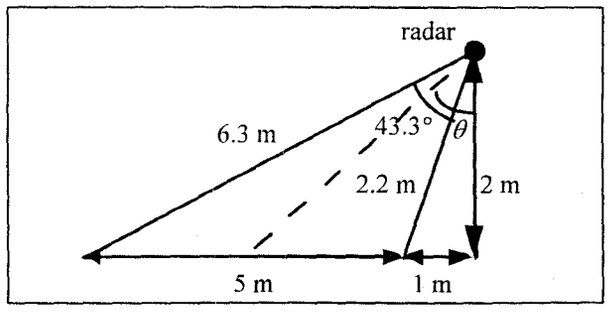

Figure 2: radar positioning

For sufficient sampling, the pulse repetition frequency (PRF) must be such that PRF > 2v/d, where v is the radar velocity and d is the antenna dimension (5 mm). The image must be formed within 1 s during which little movement is expected to occur and therefore the target scene can be regarded as stationary. So the required radar velocity is 1 m/s. To ensure adequate sampling a PRF of 3v/d should be used giving a figure of 600 Hz. The PRF should not be higher than necessary or the S/N ratio will suffer since a higher PRF results in a higher receiver noise bandwidth, as shown by the radar equation.

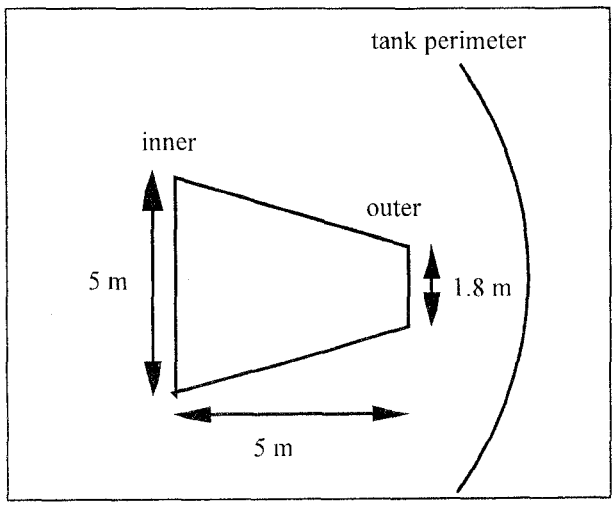

Figure 3: imaged area

Table 1 summarises the main parameters of the radar.

centre frequency	f_c	94 GHz
sweep bandwidth	B	3 GHz
pulse repetition frequency	PRF	600 Hz
sweep duration	T	1.66 ms
antenna size	d_x x d_y	7 x 5 mm^2
slant range resolution	ΔR	5 cm
azimuth resolution	Δx	3.5 mm

Table 1- Parameters of the radar

Using the single-pulse radar equation:

$$\frac{P_r}{P_n} = \frac{P_t G^2 \lambda^2 \sigma^0 A}{(4\pi)^3 R^4 F k T_0 \Delta f}$$

where P_r is the received power, P_n is the noise power, P_t is the transmitted power, G is the antenna gain, A is the area of the resolution cell at the inner edge, σ^0 is the backscattering coefficient of water, R is the maximum range, T_0 is the standard temperature (290K), Δf is the PRF and F is the noise factor, gives a S/N ratio at the inner edge of the imaged area of 25.5 dB. This is adequate, though efforts will be made in the radar construction to minimise 'plumbing' losses and to achieve the necessary noise figure (or better). Of course, S/N ratio improves considerably towards the outer edge of the imaged area where the range is smaller.

The IF bandwidth is given simply by the product of the sweep rate with the propagation delay:

$$B_{IF} = \text{sweep rate} \times \frac{2\left(R_{max} - R_{min}\right)}{c}$$

where the maximum likely range R_{max} is 7 m, the minimum likely range R_{min} is 2.2 m and the sweep rate is 3 GHz x 600 Hz. Thus the frequency components relating to the furthest and closest points from the radar are 84 kHz and 26 kHz respectively. A combination of high-pass filtering and low-pass filtering prior to the A/D card can thus be used, based on the above figures. At these low frequencies shot noise (and general 1/f noise) may be a problem.

A key component in the design is the mm-wave voltage controlled oscillator (VCO). It comprises an electronically-tuned 10V-bias Gunn oscillator with a sweep bandwidth of 3 GHz and an output power of 10 mW. The power supply to the VCO includes transient and overvoltage (crowbar) protection to safeguard the mm-wave Gunn oscillator.

The receiver, analogue-to-digital converters and subsequent processing are straightforward, because of the low bandwidths of the signals at that point. Nevertheless the receiver noise figure should be minimised for the sake of the S/N ratio; this involves the use of a low noise transistor amplifier at IF.

The design of the radar has been simplified by using separate transmit and receive antennas, and this has the additional benefit of providing a polarimetric capability. This will allow the polarimetric signatures of the water surface features to be obtained and compared with polarimetric SAR images of the ocean. The polarimetric signatures (HH, VV, HV) are, of course, obtained with successive passes of the radar rather than simultaneously. Standard gain (15 dBi) horn antennas have been chosen and will be carefully measured in an anechoic chamber.

Sync pulses will be included at the beginning of each VCO sweep so that the computer is required to act only as a data gatherer rather than being involved in the real-time control of the radar. VCO sweeping is activated when the boom passes a start marker and disabled when it passes a stop marker; sync pulses denote the beginning of each sweep. This approach simplifies the control of hardware and software.

4.2. Radar processing

The aim of the image processing is to map out the reflectivity of the terrain imaged in view as a function of range and azimuth. A rectangular algorithm will be used since it is the most common for realising SAR processing in remote sensing. Although in these experiments, the radar is very close to the water surface, the rectangular algorithm is chosen and will be handled with care as far as the geometry is concerned.

The rectangular algorithm is a two-dimensional procedure which correlates the radar signals with a computed replica of the signal which would result from observing a unit reflectivity point in isolation. The first operation of the correlation is the range compression and uses deramp compression processing. The azimuth processing then uses the pulse-to-pulse phase history of the radar relative to the target, and correlates it with the reference function (or azimuth replica) corresponding to that particular target.

In our particular application the azimuth processing will be complicated by the fact that, since the image must be formed within 1 s, the synthetic aperture is not fully formed for an imaged area of 5 m width. As a result, the azimuth resolution will change for each cell of the imaged area.

A crucial issue in the process of imaging is motion errors. They are expected to be significant: errors of

the order of $\lambda/4$ (0.8 mm at 94 GHz) would be sufficient to cause degradation of the image, so such errors need to be estimated and compensated. Especially in the Coriolis experiment, motion errors are expected to be not only significant but different with each use of the radar.

4.3. Progress in radar hardware

The first step consisted of evaluating the linearity of the VCO which is the signal source of the radar. The frequency-vs-voltage tuning characteristic of the oscillator (Gunn diode) is not perfectly linear over the radar bandwidth B. Hence the tuning characteristic has been measured with high precision (250 points for a 25V ramp) using a mm-wave spectrum analyser based in ENSTBr, France. Measurements have been carried out at different temperatures (13°C, 20°C and 25°C) using a Peltier-effect set-up to regulate the temperature of the VCO. The conclusion of these experiments is that the temperature-dependence of the VCO has to be taken into account during the radar experiments. It has been noticed that a regulation of the VCO at 25°C would be very convenient, since it was very stable (variation of a few tenth of °C) compared to lower temperature where regulation was more difficult to obtain because of VCO heating. The frequency-vs-voltage characteristic allows derivation of the required voltage-vs-time characteristic which will be stored in digital form in programmable memory, so as to linearise the sweep.

Then the IF receiver as well as the power supplies have been built and tested. The receiver exhibits a noise figure of 3.3 dB. The expected conversion loss of the mixer is only about 5 dB which results in an overall noise figure of 9 dB. This gives an improvement of 5 dB on the signal to noise ratio calculated in section 4.1.

5. LABORATORY INVESTIGATIONS

Two experiments, among others, will be carried out to study the interaction of long internal wave - short gravity/capillary wave interactions as well as the long internal wave generation and refraction.

5.1. Flume experiment

To obtain experimental evidence of blockage (when waves break), phase shift and complex phenomena in the interaction between a short surface wave and a long internal wave, solitary internal waves will be produced in a two layer medium, in a flume and imaged by the laboratory radar. The two layer system will be made of salted water under fresh water with a typical difference of density around 0.5 % hence realistically reproducing the ocean stratification. The long wave flume is 36 m long, 55 cm wide and 1.38 m high. Here the experiment will consist of generating a solitary internal wave propagating in one direction, with simultaneously short waves in the opposite direction. Typically solitary waves travel at 1 to 2 m/s and short waves at 4 to 6 cm/s. In this case, the radar is to be used as a static radar, only providing range information since it is assumed that the wave does not vary in azimuth in such a flume. It will take a sequence of snapshots of the waves each providing a one-dimensional plot of the imaged area. The radar will be mounted 3 m above the water surface with an angle of 70° giving a resolution of 5.4 cm. The set-up is shown in figure 4.

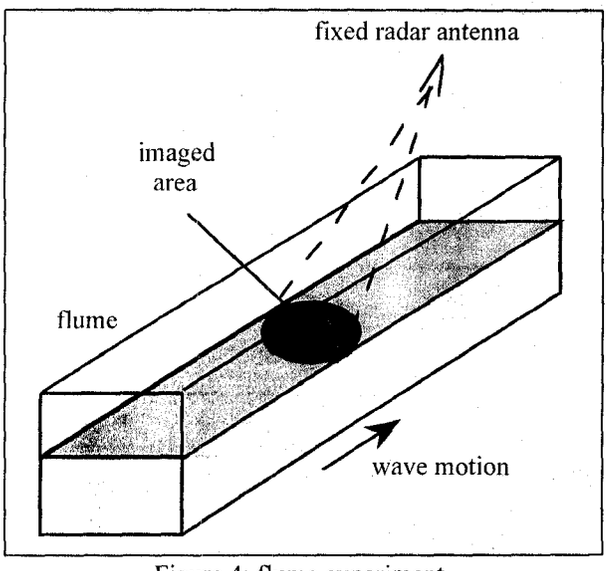

Figure 4: flume experiment

5.2. Coriolis wave-tank experiment

Long internal waves are essentially generated by the tidal flow over continental step shelves or bottom topographies. Through high-resolution SAR imagery of a two layer system in the Coriolis wave-tank, the changes in the surface wave field introduced by the moving internal wave as it passes over the shelf will be analysed. The Coriolis turntable is a 14 m diameter platform capable of rotating hence simulating the Coriolis effect due to earth rotation. A solitary internal wave generator and a step-like topography will be installed in the tank and the radar will be placed 2 m above the water surface looking over the shelf region. It will be mounted on a boom elevated by some support structure, allowing it to move at the required speed (1 m/s) to synthesise the aperture. Hence this experiment will provide a two-dimensional plot of the imaged area with information in both range and azimuth. Figure 5 shows the schematic set-up of the radar above the tank.

As mentioned earlier, motion errors are expected to be significant. The correction of these errors may be achieved by using laser interferometry. An interferometric laser would record the radar path in three dimensions with a very high resolution. Another solution is to use three corner reflector targets fixed at edges of the target scene, clear of the target area of interest, and to track their echoes through each pulse. One of these two solutions will allow the exact position of the radar to be estimated for each pulse and hence the exact azimuth reference function to remove the effect of motion errors.

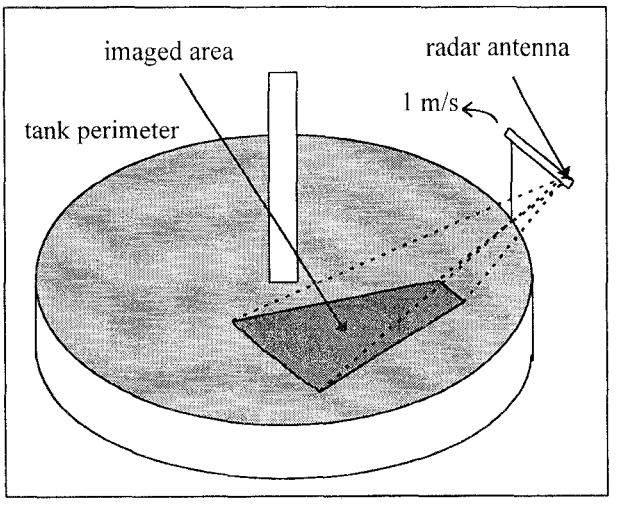

Figure 5: Coriolis wave tank experiment

6. SUMMARY

The goal of the MORSE project is, first, to gain extensive understanding on the interaction of internal waves with external ones, and then to contribute to the development of a management tool for extracting ocean information from radar signatures. This includes the following tasks: extraction of wave parameters from images, understanding of ocean images, laboratory SAR development and radar backscatter modelling.

The laboratory SAR is now well under way as much of its hardware has been built and tested. Much of the effort will be now dedicated to the radar software which will process the SAR images. This a particularly complex task not only because the resolution varies in range and azimuth but also because of the problem due to motion errors, which is a crucial issue in image processing.

The project has a home page on the world wide web. The site, known as the MDR, Morse Data Information and Documentation Repository, is being maintained by OCS. Its URL is:

http://www.compulink.co.uk/~ocs/morse/

Information on the UCL W-band radar and on the images to be obtained from the LEGI tank experiments will be kept on the MDR. When available, some example images will be put on the site.

ACKNOWLEDGMENT

This work forms part of that carried out under the CEC MAST III Contract MAS3 CT95-0027 (DG12-ESCY). The authors wish to acknowledge with thanks the support provided by the EU contribution to the funding of the project.

REFERENCES

1. Alpers W and Salusti E, 1983, "Scylla and Charibdis observed from space", J. Geoph. Res., 88, 1800-1808

2. Rufenach C and Smith C, 1985, "Observation of internal wave in LANDSAT and SEASAT imagery", Int. J. Remote Sensing, 6, 1201-1207

3. Garello R, Cariou C and Boucher J-M, 1991, "Estimation spectrale paramétrique d'images SAR de la surface de la mer", Télédétection et Gestion des Ressources, 8, 271-279

4. Grassin S and Garello R, 1996, "Spectral analysis of non-stationary ocean SAR images using the Wigner-Ville transform", Proc. IGARSS'96, Lincoln, USA, 4, 1956-1958

5. Ródenas J A and Garello R, 1996, "Detection and location of internal waves in ocean SAR images by means of wavelet decomposition analysis", Proc IGARSS'96, Lincoln, USA, 4, 1953-1955

6. Griffiths H D, 1988, "Synthetic aperture processing for full-deramp radar altimeters", Elec.Letters, 24, 371-373

7. Griffiths H D and Purseyyed B, 1989, "A radar altimeter with synthetic aperture processing", Proc. XIX European Microwave Conference, London, Microwave Exhibitions & Publishers Ltd, 281-286

8. Griffiths H D, "New ideas in FM radar", 1990, IEE Electronics & Communication Engineering Journal, 2, 185-194